Isotopic fractionation of carbon in the coccolithophorid *Emiliania huxleyi*

Dan Tchernov[1],*, David F. Gruber[2], Andrew Irwin[3]

[1]Marine Biology Department, The Leon H. Charney School of Marine Sciences, University of Haifa, Mount Carmel, Haifa 31905, Israel

[2]Department of Natural Sciences, Baruch College, City University of New York and Sackler Institute for Comparative Genomics, American Museum of Natural History, New York, NY, USA

[3]Department of Mathematics and Computer Science, Mount Allison University, Sackville, New Brunswick, Canada

ABSTRACT: Relating atmospheric CO_2 to $\delta^{13}C$ of calcifying phytoplankton is often used as a proxy to reconstruct paleo-CO_2. Therefore, a firm undertanding of how living cells fractionate carbon under different environmental conditions (known as vital effects) is necessary when interpreting $\delta^{13}C$ values. In this study, we measured the isotopic fractionation of carbon in organic matter (ε_p) in the globally distributed, bloom-forming coccolithophorid *Emiliania huxleyi* grown in continuous culture under nutrient-replete conditions with growth rate limited by light or temperature. At a constant temperature of 18°C, growth followed a hyperbolic function of irradiance. At low irradiance levels, changes in ε_p were highly correlated with growth rate. However, as growth became light-saturated, ε_p declined with increasing light intensities. When temperature was increased from 7 to 18°C at a constant photon flux density, equilibrium partial pressure CO_2 concentrations ($[pCO_2]$) decreased from 17 to 13 μM, and ε_p values declined from 25 to 19‰. As temperature was increased further to 26°C, $[pCO_2]$ declined to 10 μM and ε_p increased to 25‰. This non-linear pattern in isotopic fractionation is consistent with the induction of a carbon-concentrating mechanism at low $[pCO_2]$ that replenishes the internal inorganic carbon pool with isotopically lighter carbon. In this study, we present an empirical model that predicts this non-linear behavior, and we validate this model with experimental data. These results suggest extreme variability in the isotopic fractionation of carbon in the bulk organic pool in *E. huxleyi* that precludes the reconstruction of pCO_2 from isotopic measurements without *a priori* knowledge of temperature.

KEY WORDS: *Emiliania huxleyi* · Calcifying phytoplankton · Isotopic fractionation of carbon · Vital effects · Paleo-CO_2 reconstruction · Temperature · Carbon-concentrating mechanism

INTRODUCTION

Farquhar et al. (1982) introduced a model relating the isotopic composition of organic carbon in terrestrial C3 plant leaves to the concentration of CO_2 in air. The model assumes a diffusive flux of CO_2 from the atmosphere to the site of carbon fixation. Hence, intracellular $[CO_2]$ is always less than (or at most, equal to) that in air, and their model predicts that a leaf becomes more ^{13}C enriched when atmospheric $[CO_2]$ decreases. The basic concept of relating $[CO_2]$ to $\delta^{13}C$ or organic matter was subsequently adopted by the oceanographic community to reconstruct paleo-CO_2 from measurements of the carbon isotopic composition of organic matter in marine phytoplankton (Rau et al. 1982, Jasper & Hayes 1990, Freeman & Hayes 1992, Rau 1994, Pagani et al. 1999, 2002, Bolton et al. 2012). This proposal has led to numerous theoretical, laboratory and marine phytoplankton field studies, examining both environmental and physiological controls on the fractionation of carbon isotopes (Laws et al. 1995, Wolf-Gladrow et al. 1999, Riebesell et al. 2000, Rost et al. 2006, Brutemark et al. 2009). However, these studies revealed that the phytoplankton carbon isotopic composition is not simply a function of ambient aqueous CO_2 levels

(CO_2(aq)), and several vital factors also play a role. These factors include growth rate, cell size, cell wall permeability, taxonomic composition and, critically, the ability of the cell to actively assimilate carbon, instead of strictly relying on passive diffusion (Keller & Morel 1999, Riebesell et al. 2000, Rost et al. 2002, Raven et al. 2011).

Based on chemostat culturing experiments, where growth rate was controlled by nitrate limitation, Laws et al. (1995) suggested that the effective isotopic carbon fractionation (ε_p) in marine autotrophs is inversely linearly related to the ratio of diffusive CO_2(aq) supply into the cell and hence carbon fixation (expressed as specific growth rate, μ). Subsequent experiments suggested that this relationship only applies at low μ:[CO_2] ratios, i.e. when CO_2(aq) concentrations are relatively high and/or growth rates are low. Under such conditions, inorganic carbon fluxes from the bulk media into the cell can be assumed to follow Fickian diffusion (e.g. Wolf-Gladrow & Riebesell 1997). However, as photosynthetic (or, in the steady state, growth) rates increase, inorganic carbon is actively transported into the cell, rendering the inverse relationship between ε_p and μ:[CO_2] inapplicable (Laws et al. 1998). The exact μ:[CO_2] ratio, however, varies among phytoplankton species depending on their cell shape and size (expressed as the ratio between the volume to surface area of the cell), which influences the total diffusive carbon flux into the cell (Laws et al. 1998).

In this study, we investigated the carbon isotopic fractionation in the globally distributed, bloom-forming coccolithophorid *Emiliania huxleyi* (Iglesias-Rodriguez et al. 2002, Brutemark et al. 2009), as a species that produces biomarker lipids (alkenones). The isotopic signature of these alkenones has been used to reconstruct paleoceanographic $\delta^{13}C_{org}$ records (Jasper & Hayes 1990, Pagani et al. 1999, Bolton et al. 2012). In contrast to experiments conducted by Laws et al. (1995, 1998), we grew *E. huxleyi* in turbidostats, where growth rates are not limited by nutrients, but instead by light or temperature (e.g. Falkowski 1984a,b, Sukenik et al. 1987). These 2 culturing conditions (turbidostat and chemostat) are fundamentally different and using chemostats, cells never attain their maximum specific growth rate as the physiological restriction on growth depends upon what nutrient is selected to be limiting. For example, the limitation of dissolved inorganic nitrogen leads to decreased protein synthesis, especially plastid proteins and the carbon-fixing enzyme ribulose 1,5-bisphosphate carboxylase (RuBisCO). As intracellar RuBisCO concentrations strongly deter-

mine the rate of light-saturated carbon fixation (Sukenik et al. 1987), nitrogen-limited chemostat cultures can lead to an unintentionally imposed relationship between [CO_2] and isotopic fractionation of carbon. In contrast, turbidostat growth rates can be manipulated without nutrients being limiting. In this study, we examined 2 types of growth limitation: light limitation at a constant temperature (18°C, the mean temperature of the upper ocean), and temperature limitation at a constant growth irradiance. Our results clearly suggest that the relationship between ε_p and μ:[CO_2] is non-linear over the full range of growth rates. Based on our experimental results, we propose a new, quasi-mechanistic model, based on the active transport of inorganic carbon, which empirically accounts for this observed pattern of carbon isotopic fractionation.

MATERIALS AND METHODS

Culture conditions

Clonal cultures of *Emiliania huxleyi* strain CCMP 374 (isolated from the Gulf of Maine in 1989) were grown in a turbidostat system at the Rutgers University Institute of Marine and Coastal Sciences in nutrient-replete continuous cultures with 24 h illumination (Falkowski 1984a, Post et al. 1984). Constant cell density was maintained by continuously monitoring the attenuation of light at 650 nm (coupled LED/photodiode) via feedback from a microprocessor to a pump-controlled nutrient reservoir. As cell densities exceed a preset value, the pump is turned on and dilutes the culture; the dilution volumes are monitored and the growth rate is calculated hourly. The culture chamber consisted of a water-jacketed 3.2 l cylinder with light provided by high-intensity fluorescent tubes. For light-limiting growth rate measurements, light intensities ranged from 9 to 286 µE m^{-2} s^{-1} and the culture was kept at 18°C, while for temperature-limited growth measurements, temperatures ranged from 7 to 26°C with a measurement uncertainty of ±0.5°C. We constrained temperature-dependent experiments to a minimal variation in light intensity (80 ± 5 µmol photons m^{-2} s^{-1}) to minimize the effects of varying photosynthetic flux density (PFD) on our results.

Media was prepared from New Jersey coastal seawater with a salinity of 31 PSU and nutrients enriched to f/50 (Guillard & Ryther 1962). Growth rates (cell divisions per day) were calculated from culture dilution rate, and adjusted for any changes in

cell density checked by daily cell counts on a Coulter Counter. Cell densities were maintained at an optically thin concentration of $3 \pm 0.5 \times 10^5$ cells ml^{-1}. The cultures were bubbled continuously with air pumped from an intake outside of the laboratory building to avoid the pCO$_2$ variability in a closed room with recirculated air. pCO$_2$ in the culture chamber was measured continuously using a LI-COR IR monitoring system (Stoll et al. 2002). The cultures were pre-adapted to each experimental condition for approximately 6 generations before collection of samples. Cell samples were collected simultaneously for measurements of cell density, calcification rate and carbon isotope composition of the organic fraction and medium solution.

Carbon fixation and calcification rates

Estimates of carbon fixation rates are based on daily measurements of culture growth rates and assuming a constant cell radius of 3.5 μm using the equation:

$$\text{C-fixation rate } = \text{ }^4/_3\, \pi\, r^3 \times 0.5968\, \mu \qquad (1)$$

where r is the average cell radius and μ is the daily growth rate.

The amount of calcification per cell was determined from measurements of calcite recovered from a given culture volume divided by the number of cells in that culture volume following the procedure outlined in Stoll et al. (2002). The amount of calcite per cell varied greatly, from 5 to 52 pg calcite cell^{-1}. Given steady-state growth, the product of calcite per cell and growth rate (cell divisions per day) yields the calcification rate for the culture. Because growth rate is a factor in the calculation of calcification rate, and because calcification per cell generally increases with growth rate, there is a strong correlation between growth rate and calcification rate ($r^2 = 0.8$ for 18°C samples).

Carbon isotope measurements

Samples for particulate organic carbon (POC) δ^{13}C$_{org}$ analyses were filtered from 50 ml culture solution on pre-combusted 13 mm Gelman A/E glass filters (pre-combusted for 4 h at 500°C). The filters were fumed overnight in a dissector filled with 1 ml of 12 N HCl to remove the coccolith calcite. Subsequently, the fumed filters were left in the fume hood to allow the acid to evaporate, wrapped in aluminum

foil and stored in the freezer. Measurements of δ^{13}C$_{org}$ were performed in 2 different laboratories. The first set of phytoplankton samples from the variable light constant temperature experiment was analyzed using a Europa mass spectrometer (Sam Wainright laboratory, Rutgers University). Samples from the second experiment of constant light and variable temperature were analyzed using a Finnigen 251 mass spectrometer (UC Santa Cruz Stable Isotope Laboratory).

Water samples for the analysis of δ^{13}C in dissolved inorganic carbon (DIC) were filtered using syringe-mounted 0.2 μm Gelman Acrodisc filters. Samples of approximately 8 ml of water were sealed in pre-combusted vials, pre-poisoned (with 40 μl saturated HgCl$_2$), and flushed with nitrogen gas. δ^{13}C$_{DIC}$ were analyzed at the Sam Wainright laboratory. Isotopic fractionation during carbon fixation (ε_p) was calculated from δ^{13}C$_{org}$ isotopic composition relative to δ^{13}C$_{DIC}$ isotopic composition of the growth medium using a modified version of Freeman & Hayes' (1992) equation:

$$\varepsilon_p \text{ } = \text{ } \frac{\delta^{13}C_{DIC} - \delta^{13}C_{POC}}{1 + \dfrac{\delta^{13}C_{POC}}{1000}} \qquad (2)$$

Note that this equation differs from the original one as we compare the carbon isotopic composition of the organic matter to that of DIC rather than to CO$_2$(aq). This was performed as CO$_2$(aq) is not the sole source of carbon into the cell.

RESULTS

At constant temperature ($T = 18 \pm 1$°C), the relationship between growth rate (μ) and PFD was hyperbolic, with an increase of μ from 0.1 to 1.6 d^{-1} in response to increasing light levels from 9 to 286 μmol m^{-2} s^{-1} (Fig. 1A, open symbols outside the dashed rectangle). Under these conditions, μ:[CO$_2$] ratios are linearly dependent on growth irradiance over the entire range of growth rates (Fig. 1C). Varying the temperature from 7 to 26°C at near-constant PFD (80 μmol photons m^{-2} s^{-1}) resulted in an increase in growth rate from 0.2 to 1.4 d^{-1} (Fig. 1B). Temperature-induced variations in μ exhibited logarithmic behavior with growth rates leveling off at 18°C, and at the lower end of the temperature range μ was significantly attenuated. There was an inverse correlation between μ and CO$_2$ concentrations in the growth medium (CO$_2$ concentration ranging from 14 to 18.5 μM; $r = -0.86$, $p < 0.001$; Table 1), and CO$_2$ solubility decreased with increasing temperature. Conse-
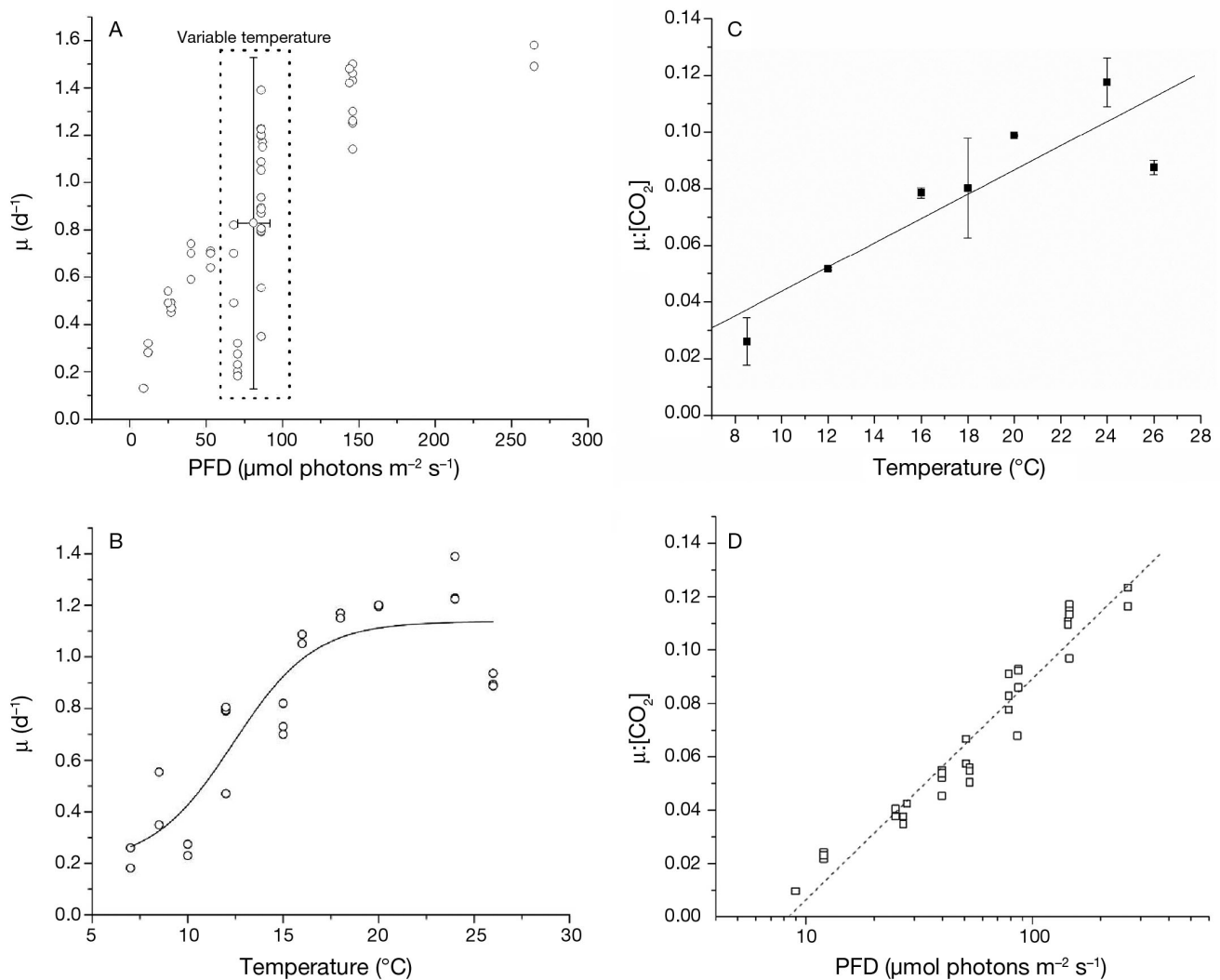
Fig. 1. (A) Relationship between daily growth rate (μ) and photosynthetic flux density (PFD). Symbols within the dashed rectangle represent cultures grown at 7–26°C, while symbols outside the rectangle represent cultures grown at 18°C. One symbol in the dashed rectangle has SD error bars and represents the mean range of all of the growth rates measured under variable temperature, and shows the high variation under such conditions. (B) Relationship between μ and temperature. The sigmoidal (Boltzmann) fit ($R^2 = 0.807$) is given. (C) Relationship between μ:$[CO_2]$ and temperature. Linear regression curve is given ($R^2 = 0.842$). (D) Relationship between μ:$[CO_2]$ and PFD (plotted on a log scale). Linear regression curve is given ($R^2 = 0.97$)

quently, the μ:$[CO_2]$ ratios showed a positive linear relationship with temperature, except at our highest temperature (26°C), where the ratio was anomalously low (Fig. 1C).

Carbon fixation rate also showed positive dependence on temperature ($r = 0.88$, $p < 0.001$; Table 1), and we found a 10-fold increase in carbon fixation rate from 7 to 24°C, with a significant decrease at 26°C (where μ is low, $p < 0.05$). Carbon fixation rates were inversely correlated with CO_2 concentration ($r = -0.92$, $p < 0.001$; Table 1). At a constant temperature (18°C), a linear variation in μ:$[CO_2]$ occurred as a logarithmic function of light intensity (Fig. 1D).

When ε_p is plotted versus μ:$[CO_2]$ (Fig. 2) for cultures grown at 70–86 μmol photons m^{-2} s^{-1}, the higher range of CO_2 concentrations (above 15 μM, see vertical arrow) had lower μ:$[CO_2]$ ratios and ε_p was inversely correlated with μ:$[CO_2]$ ($r = -0.95$, $p < 0.001$). Under such high concentrations, inorganic carbon (Ci) uptake may still depend on diffusion; however, under lower $[CO_2]$ and higher μ:$[CO_2]$ we observed no dependency of ε_p on μ:$[CO_2]$. ε_p decreased from 25.2 to 19.3‰, but then when $[CO_2]$ rose above 13 μM, ε_p increased back to 25.2‰ (Fig. 3A). A similar trend was captured with ε_p plotted versus temperature (Fig. 3B).

Table 1. Data collected from chemostat experiments. PFD: photosynthetic flux density; μ: specific growth rate; $CO_2(aq)$: aqueous CO_2; POC: particulate organic carbon; DIC: dissolved inorganic carbon; ε_p: isotopic fractionation during carbon fixation; ND: not determined

| Date (mm/dd/yy)	Medium	Temp. (°C)	PFD (μmol photons m^{-2} s^{-1})	μ (d^{-1})	Chl a conc. (pg chl a cell^{-1})	C fixation rate (μm^3 d^{-1})	[CO_2(aq)] (μM)	μ:[CO_2]	POC δ^{13}C (‰)	DIC δ^{13}C (‰)	[CO_2(aq)] δ^{13}C (‰)	ε_p (CO_2)	ε_p (DIC)
8/26/99	f/50	7	71	0.26	ND	3.6	18.5	0.014	−27.2	2.3	−8.7	19.1	30.3
9/8/99	f/50	7	71	0.18	0.15	2.5	18.5	0.010	−26.0	2.3	−8.6	17.8	29.0
1/3/01	f/50	8.5	86	0.35	ND	4.8	17.3	0.020	−25.7	−1.0	−11.8	14.4	25.4
12/19/00	f/50	8.5	86	0.55	ND	7.7	17.3	0.032	−25.3	−1.0	−11.8	13.9	25.0
8/6/99	f/50	10	71	0.27	ND	3.8	16.2	0.017	−26.8	0.6	−10.0	17.3	24.6
8/11/99	f/50	10	71	0.23	0.13	3.2	16.7	0.014	−25.8	1.5	−9.1	17.1	27.9
7/28/99	f/50	12	71	0.47	0.19	6.5	16.5	0.029	−24.8	0.2	−10.1	15.0	25.6
10/21/00	f/50	12	86	0.79	ND	10.9	15.4	0.051	−22.0	−1.0	−11.3	10.9	21.4
11/25/00	f/50	12	86	0.79	ND	11.0	15.4	0.051	−22.6	−1.0	−11.3	11.5	22.1
11/29/00	f/50	12	86	0.81	ND	11.1	15.4	0.052	−23.5	−1.0	−11.3	12.5	23.1
719199	f/50	15	68	0.73	0.14	10.1	14.2	0.051	−20.6	−0.2	−10.2	10.6	18.1
7/14/99	f/50	15	68	0.82	0.17	11.3	15.1	0.054	−20.1	0.3	−9.7	10.5	20.7
7/20/99	f/50	15	68	0.70	0.13	9.7	15.1	0.046	−21.2	−0.7	−10.7	10.8	21.0
9/22/00	f/50	16	86	1.09	ND	15.0	13.6	0.080	−20.5	−1.0	−10.9	9.8	19.9
9/28/00	f/50	16	86	1.05	ND	14.5	13.6	0.077	−21.2	−1.0	−10.9	10.5	20.6
5/10/99	f/50	18	87	1.17	ND	16.2	12.6	0.093	−20.5	−0.1	−9.7	11.1	20.9
5/11/99	f/50	18	87	1.17	ND	16.2	12.7	0.092	−21.9	−0.2	−9.8	12.4	22.2
5/12/99	f/50	18	87	1.15	0.15	15.9	13.4	0.086	−21.9	−0.1	−9.7	12.4	22.3
9/19/00	f/50	20	86	1.20	ND	16.5	12.1	0.099	−20.7	−1.0	−10.4	10.5	20.1
9/25/00	f/50	20	86	1.20	ND	16.6	12.1	0.099	−22.3	−1.0	−10.4	12.2	21.8
10/19/00	f/50	24	86	1.23	ND	17.0	10.9	0.113	−22.5	−1.0	−9.9	12.9	22.0
10/30/00	f/50	24	86	1.22	ND	16.9	10.9	0.112	−22.6	−1.0	−9.9	12.9	22.1
11/18/00	f/50	24	86	1.39	ND	19.2	10.9	0.128	−22.1	−1.0	−9.9	12.5	21.6
12/23/00	f/50	26	86	0.89	ND	12.4	10.4	0.086	−24.3	−1.0	−9.7	15.0	23.9
1/4/01	f/50	26	86	0.94	0.23	13.0	10.4	0.090	−27.6	−1.0	−9.7	18.4	27.3
1/10/01	f/50	26	86	0.89	0.21	12.3	10.4	0.086	−24.9	−1.0	−9.7	15.6	24.5
3/2/00	f/50	18	9	0.13	0.23	1.8	13.2	0.010	−25.2	−1.5	−11.2	14.4	24.3
4/17/00	f/50	18	12	0.32	0.20	4.4	13.2	0.024	−21.8	−1.3	−11.0	11.1	20.9
5/11/00	f/50	18	12	0.28	0.20	3.9	13.0	0.022	−22.4	−0.4	−10.0	12.7	21.9
5/22/00	f/50	18	12	0.32	0.20	4.4	13.9	0.023	−22.2	−0.1	−9.7	12.7	21.6
2/10/00	f/50	18	25	0.49	0.19	6.8	13.2	0.037	−22.6	−1.4	−11.0	11.8	21.7
2/15/00	f/50	18	25	0.54	0.18	7.5	13.3	0.041	−22.6	−1.4	−11.0	11.8	21.7
3/30/99	f/50	18	27	0.49	ND	6.8	13.0	0.038	−30.6	−2.9	−12.6	18.6	28.5
4/1/99	f/50	18	27	0.45	ND	6.2	13.0	0.035	−32.0	−3.5	−13.1	19.5	29.5
4/7/99	f/50	18	27	0.47	ND	6.5	13.6	0.035	−32.9	−3.2	−12.8	20.8	30.7
3/11/99	f/50	18	40	0.74	0.15	10.2	13.4	0.055	−29.1	−2.2	−11.9	17.8	27.7
3/21/99	f/50	18	40	0.70	0.16	9.7	13.0	0.054	−28.0	−2.2	−11.8	16.7	26.6
3/28/99	f/50	18	40	0.59	ND	8.2	13.0	0.045	−29.5	−2.4	−12.0	18.0	27.9
6/7/00	f/50	18	53	0.64	0.21	8.8	12.7	0.050	−21.1	−1.5	−11.2	10.2	20.6
6/15/00	f/50	18	53	0.71	0.21	9.8	12.7	0.056	−20.9	0.9	−8.7	12.4	20.3
6/22/00	f/50	18	53	0.70	0.20	9.7	12.8	0.055	−20.7	0.7	−8.9	12.1	20.1
9/12/00	f/50	18	86	0.87	ND	12.0	12.8	0.068	−19.9	−1.0	−10.6	9.4	19.3
5/15199	f/50	18	144	1.48	ND	20.5	13.4	0.110	−21.7	0.0	−9.6	12.3	22.1
5/18/99	f/50	18	144	1.42	ND	19.6	13.0	0.109	−21.2	0.4	−9.2	12.2	22.1
1/4/99	f/50	18	146	1.30	0.18	18.0	9.2	0.142	−23.5	−0.6	−10.3	13.6	23.4
1/6/99	f/50	18	146	1.25	0.16	17.3	9.4	0.133	−22.6	−0.1	−9.8	13.2	23.0
1/11/99	f/50	18	146	1.25	0.13	17.3	8.7	0.144	−22.0	−0.5	−10.1	12.1	22.0
1/12/99	f/50	18	146	1.14	0.14	15.8	8.0	0.142	−21.9	−0.5	−10.1	12.0	21.8
2/11/99	f/50	18	146	1.26	ND	17.4	11.5	0.109	−24.0	−0.9	−10.6	13.7	23.6
2/15199	f/50	18	146	1.43	0.15	19.8	14.8	0.096	−23.3	−2.2	−11.8	11.7	21.6
2/16/99	f/50	18	146	1.46	0.17	20.2	12.7	0.115	−24.2	−1.9	−11.6	12.9	22.8
2/17199	f/50	18	146	1.50	0.16	20.7	12.4	0.121	−24.3	−1.7	−11.3	13.3	23.2
8/9/00	f/50	18	265	1.58	ND	21.8	12.8	0.123	−17.1	2.4	−7.2	10.1	16.4
9/5/00	f/50	18	265	1.49	ND	20.6	12.8	0.116	−20.4	1.5	−8.1	12.5	19.8
2/28/00	f/2	18	9	0.10	0.23	1.3	13.6	0.007	−24.2	−1.3	−10.9	13.6	21.1
3/20/00	f/2	18	9	0.12	0.21	1.6	13.4	0.009	−25.2	−1.3	−10.9	14.6	23.4
4/5/00	f/2	18	12	0.31	0.16	4.3	12.9	0.024	−21.9	−0.5	−10.1	12.1	17.9
4/13/00	f/2	18	12	0.33	0.18	4.5	13.0	0.025	−22.6	−0.4	−10.0	12.9	22.8
4/19/00	f/2	18	12	0.35	0.20	4.9	13.1	0.027	−23.4	−1.3	−11.0	12.7	21.6
5/17/00	f/2	18	12	0.26	0.19	3.6	13.2	0.020	−24.4	−1.5	−11.1	13.6	24.0
1/10/00	f/2	18	25	0.43	0.18	5.9	13.0	0.033	−23.2	−1.1	−10.7	12.8	21.3
1/18/00	f/2	18	25	0.38	0.18	5.3	13.1	0.029	−22.6	−0.4	−10.1	12.9	22.7
2/8/00	f/2	18	25	0.50	0.18	6.9	12.8	0.039	−22.0	−1.2	−10.8	11.5	21.3
2/17/00	f/2	18	25	0.55	0.16	7.7	13.3	0.041	−22.3	−1.3	−10.9	11.7	21.5
11/16/99	f/2	18	71	0.88	0.19	12.2	13.0	0.068	−21.6	0.1	−9.5	12.3	22.1
11/30/99	f/2	18	71	1.03	0.18	14.3	12.0	0.086	−21.0	0.1	−9.5	11.7	21.4
12/7/99	f/2	18	123	1.16	0.19	16.0	12.8	0.090	−20.4	0.1	−9.5	11.1	20.9
12/20/99	f/2	18	123	1.19	0.18	16.4	12.8	0.093	−19.9	0.2	−9.4	10.8	20.6
8/3/00	f/2	18	265	1.41	ND	19.5	12.8	0.110	−19.7	1.5	−8.1	11.8	19.0
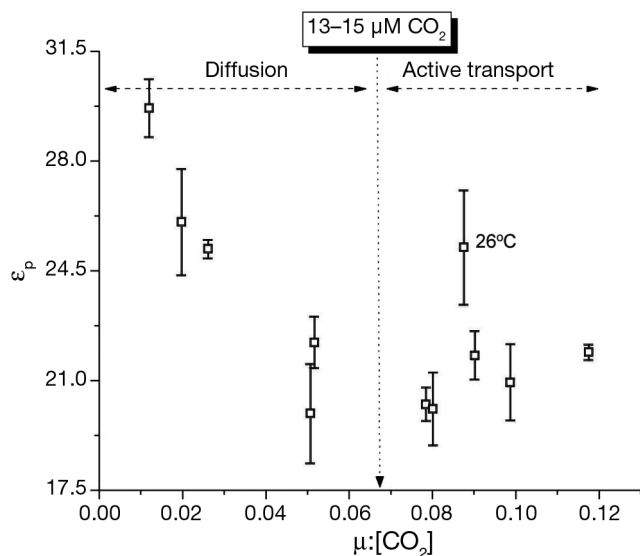
Fig. 2. Relationship between isotopic fractionation during carbon fixation (ε_p) and μ:[CO_2] for cultures grown on f/50 medium under illumination of 70–86 µmol photons m^{-2} s^{-1}. When CO_2 concentrations were high (above 15 µM) and μ:[CO_2] values were low, ε_p was inversely correlated with μ:[CO_2] ($R^2 = 0.9015$), suggesting that Ci uptake depended on diffusion. When [CO_2] was low and μ:[CO_2] was high, there was no dependency of ε_p on μ:[CO_2]

We noted a decrease of 5‰ in ε_p as PFD increased from 1 to 23 µmol photons m^{-2} s^{-1} under constant temperature (18°C) (Fig. 4). The relationship between ε_p as a function of light- and temperature-controlled variations in μ:[CO_2] are plotted and compared with data from N- and CO_2-limited studies on the same species (Fig. 5). The results clearly show that for both temperature- and irradiance-limited growth, the relationship between ε_p and μ:[CO_2] was linear at low values of μ:[CO_2] but as μ:[CO_2] increases above ca. 0.065, ε_p became constant.

DISCUSSION

Results of our 2 sets of turbidostat experiments exhibit similar relative trends of ε_p versus μ:[CO_2] for both irradiance- and temperature-limited growth, albeit with a ca. 4% offset between growth- and temperature-limited cultures (Fig. 5). The data shown in Figs. 3 & 5 suggest 2 basic patterns. At μ:[CO_2] ratios below 0.065 µmol kg^{-1} d^{-1}, ε_p is inversely linearly dependent on μ:[CO_2] ($\varepsilon_p = -140.6$ [μ:CO_2] + 24.6, $r^2 = 0.98$). Above 0.065 µmol kg^{-1} d^{-1}, there is no discernible trend between ε_p and μ:[CO_2]. These results are consistent with the study of Laws et al. (1997), who found an inverse linear relationship between ε_p
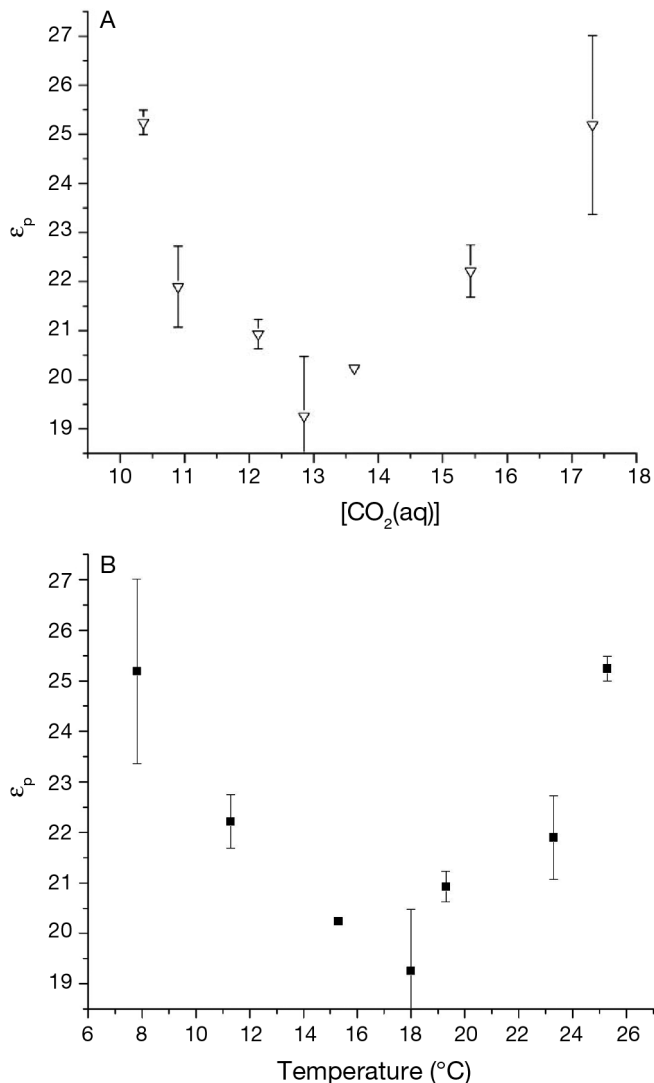
Fig. 3. (A) Relationship between isotopic fractionation during carbon fixation (ε_p) and [CO_2(aq)]. (B) Relationship between ε_p and temperature. The data are from the same experiment in which cultures were grown on f/50 medium under illumination of 70–86 µmol photons m^{-2} s^{-1}. Error bars represent ±1 SD

and μ:[CO_2], but other studies suggest that this relationship applies only to CO_2 concentrations higher than 13 µmol kg^{-1} (Laws et al. 1998, Burkhardt et al. 1999b, Keller & Morel 1999). As growth rates in their chemostat experiments were relatively low, this threshold concentration may be an underestimate. At the low μ:[CO_2] range, our data from the variable light, constant temperature experiment are consistent with data obtained by Bidigare et al. (1997) in a chemostat culture study of 2 *Emiliania huxleyi* clones, BT6 and B92/11 ($\varepsilon_p = -140.3$ μ:[CO_2] + 24.8, $r^2 = 0.79$). The results from our second experiment
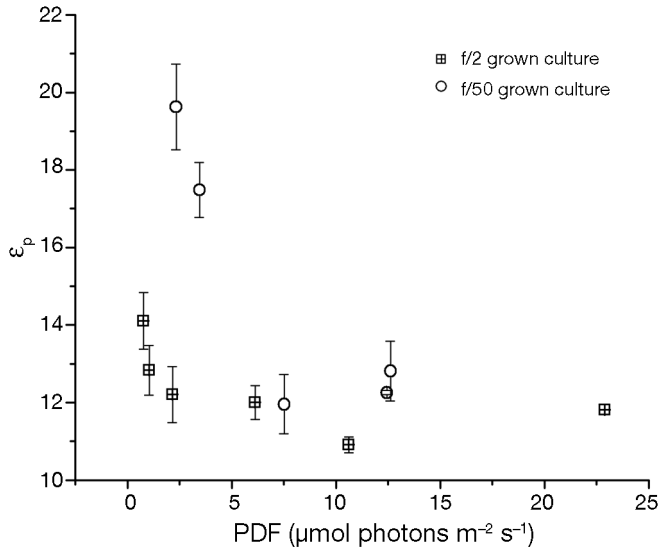
Fig. 4. Relationship between isotopic fractionation during carbon fixation (ε_p) and photosynthetic flux density (PFD) at constant temperature (18°C). Cultures were grown in f/2 and f/50 illuminated with cool white light of 0–25 µmol photons m^{-2} s^{-1}. ε_p decreases in 5‰ as PFD increases from 0 to 25 µmol photons m^{-2} s^{-1}. Error bars represent ±1 SD
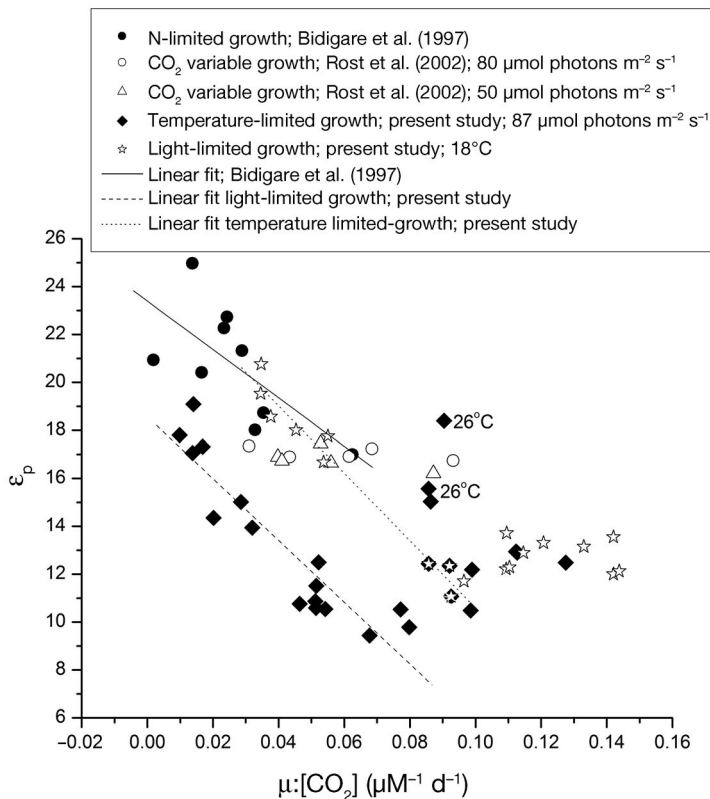
Fig. 5. Comparison of the data on the relationship between isotopic fractionation during carbon fixation (ε_p) and µ:[CO$_2$]. Data are from Bidigare et al. (1997), Rost et al. (2002) and the present study

(variable temperature, constant light) show similar relative trends, i.e. an inverse linear relationship at low µ:[CO$_2$] levels ($\varepsilon_p = -129$ µ:[CO$_2$] + 18.6, r^2 = 0.92), but there was no trend at the higher levels. Based on this pattern, we broadly define 2 major regimes that govern the isotopic fractionation: a diffusive regime and an active transport regime.

Temperature effects on ε_p

Our data suggest that the relationship between carbon isotopic fractionation and growth is highly non-linear and is strongly influenced by light and temperature. From our data, we conclude that at cold temperatures, when CO$_2$ concentrations are high (20–13 µM) yet growth rates are low, the diffusion-based (Laws et al. 1997) model is applicable and that variations in ε_p can be explained simply by the ratio of CO$_2$ demand to supply (i.e. µ:[CO$_2$]) (Fig. 2). This explanation was suggested by Laws et al. (1997) and the relationship is only applicable at CO$_2$ concentrations higher than ~13 µmol kg^{-1} (Laws et al. 1998, Burkhardt et al. 1999a, Keller & Morel 1999, Raven et al. 2012). This applies as long as enough CO$_2$ diffuses into the cell to accommodate the demand for carbon fixation. At high temperatures, when µ is high and CO$_2$ concentration is lower than 13 µmol kg^{-1}, the demand for carbon is too high to be simply supplied by diffusion.

CO$_2$-concentrating mechanism and massive carbon cycling

Several advancements have been made in elucidating carbon utilization mechanisms. Among the discoveries is the CO$_2$ concentrating mechanism (CCM) (Badger et al. 1980, Kaplan et al. 1980). The CCM enables an organism to accumulate and retain high intracellular concentrations of Ci. The Ci is maintained in the cytoplasm, mostly as HCO$_3^-$ to minimize CO$_2$ leaks. HCO$_3^-$ is actively transported to a designated seclusion body (pyrenoids in eukaryotes and carboxysomes in cyanobacteria). In haptophytes, the pyrenoid is either immersed in the chloroplast or extended from it (Edvardsen et al. 2000). The low pH combined with carbonic anhydrase activity inside the organelle ensures high [CO$_2$] and a low O$_2$:CO$_2$ ratio. Therefore, RuBisCO that is located in these seclusion bodies can operate well within its kinetic limitations (Kaplan & Reinhold 1999, Raven et al. 2012, and references therein).

The discovery of the CCM contradicted the passive diffusion models of carbon uptake and, subsequently, active transport pathways that included HCO_3^- uptake were found (Lucas 1978, Lucas & Nuccitelli 1980, Miller & Colman 1980, Kaplan 1981, Espie & Canvin 1987, Espie & Kandasamy 1992, Raven et al. 2012). Two methods were used to measure $CO_2:HCO_3^-$ uptake ratios. A membrane inlet mass spectrometry technique (Badger et al. 1994) and the isotope disequilibrium technique first described by Volokita et al. (1984) (modified by Tortell & Morel 2002) both provide supporting evidence for the active transport hypothesis and quantitative data.

CCM is also an essential physiological characteristic found in most studied phytoplankton species, including *E. huxleyi* (Nimer & Merrett 1996, Tchernov et al. 2003, Raven et al. 2012). Coccolithophores are able to incorporate DIC into an internal pool that is 13- to 16-fold (in *E. huxleyi* EH2) more concentrated than the external environment (Shiraiwa 2003). However, there is a wide variation in the kinetic properties of DIC utilization (apparent k_m values) between different species and under different conditions (Badger 1987, Sekino & Shiraiwa 1994, Nimer et al. 1995, Nimer & Merrett 1996, Sekino et al. 1996, Raven et al. 2012). Shiraiwa (2003) suggested that under low CO_2 concentrations *E. huxleyi* EH2 recycles its coccoliths as a source of carbon that is later carboxylased by RuBisCO. However, Sekino & Shiraiwa (1994) demonstrated that CO_2 was the dominant Ci species carboxylated in the very same *E. huxleyi* species. Hence, only active CO_2 uptake is possible if the internal DIC concentration inside the cytosol is 13- to 16-fold higher than in the external environment at physiological pH.

An additional component of the CCM is massive carbon cycling (MCC) (Tchernov et al. 1997, 2001, 2003, Huertas et al. 2000a). MCC is defined as light-dependent influx and efflux of inorganic carbon, independent from carbon fixation. These fluxes can vary in magnitude between 0- and 5-fold of saturated photosynthetic rates. Several authors were able to calculate a net influx of HCO_3^- and measure a concomitant net efflux of CO_2 while producing photosynthetic oxygen (Sukenik et al. 1997, Tchernov et al. 1997, Huertas et al. 2000a).

The model suggested by Keller & Morel (1999) is the first to incorporate the effect of active HCO_3^- uptake on carbon isotope fractionation (of ε_p) in organic carbon. However, this and other models do not include significant HCO_3^- efflux (Keller & Morel 1999) or any type of active exchange of DIC with the

environment (Rost et al. 2002). Most models consider a CO_2 leak as the only source of Ci efflux (Keller & Morel 1999), which is inconsistent with data from laboratory experiments, indicating that in most species HCO_3^- is the dominant species that effluxes out of the cells (Kaplan & Reinhold 1999, Tchernov et al. 2001, 2003). More importantly, the magnitude of the influx and efflux rates is underestimated by the models (Keller & Morel 1999) and contradicts much of the experimental data at hand (Tchernov et al. 1997, 2001, 2003, Kaplan & Reinhold 1999, Huertas et al. 2000b).

Effect of CCM and MCC on ε_p in *E. huxleyi*

In this study, when temperature exceeded 18°C, growth rate remained relatively stable (0.8–1.2 μ d^{-1}) (Fig. 1B). The maximum exchange between the Ci pool and the medium occurred when the lowest CO_2 concentration (maximal temperature) was reached (Fig. 3), depleting the Ci pool of ^{13}C, thus contributing to lighter $\delta^{13}C$ organic composition. The combination of all factors contributing to the final $\delta^{13}C$ composition of the algae led to the events shown in Fig. 3A: at low temperatures and high CO_2 concentrations, the rate of carboxylation was low (Table 1). The rate of MCC is low due to the low CCM activity. The CCM is only minimally active due to the high CO_2 concentration. This is a consequence of the low demand for CO_2 at the carboxylation site that is coupled with high ambient concentrations of CO_2 and results in downregulation of the CCM (Badger et al. 1978, 1980, Kaplan et al. 1980, Kaplan & Reinhold 1999, Raven et al. 2011, 2012). As temperature increases, CO_2 concentrations gradually drop, with a simultaneous increase of carboxylation rates (Table 1), and the CCM becomes more active as the activation CCM genes are strongly correlated with ambient CO_2 concentrations (Badger et al. 1978, 1980, Kaplan et al. 1980, Kaplan & Reinhold 1999). Therefore, we would expect a more vigorous activity of the CCM as temperature increases and CO_2 concentration decreases. As the demand for DIC increases and CO_2 concentration outside the cell decreases (Fig. 3A), the DIC pool becomes gradually more dominant and the supply of Ci to the carboxylation site will no longer be limiting. As a result, the fractionation rate of RuBisCO can potentially increase (higher ε_p). We observed a gradual increase in ε_p as temperature rose and the ambient CO_2 concentration dropped below 13 μM (Fig. 3). This change can be attributed to an enhancement of both

CCM and MCC activity, introducing more ^{12}C (light carbon) available for carboxylation (Fig. 3). The latter exceeds the increase in growth rate (Fig. 1B) and carbon demand as portrayed by carbon fixation rates (Table 1).

The $CO_2:HCO_3^-$ uptake ratio can shift the carbon isotopic composition of POC due to the 9‰ difference between these 2 Ci species. However, even if we assume 100% HCO_3^- uptake, this will still enrich the Ci pool with relatively light carbon as RuBisCO fractionation (–22 to –29‰) creates a much heavier Ci product that is diffusing back to the cytoplasmatic DIC pool. Therefore, the $CO_2:HCO_3^-$ uptake ratio determines only the extent of replenishment of the Ci pool with lighter carbon. Nevertheless, we do not expect this relatively minor change in CO_2 concentration to cause a large shift in the $CO_2:HCO_3^-$ uptake ratio. From previous studies, we know that the CCM creates a massive CO_2 influx because it keeps the internal CO_2 concentration lower than its surroundings (Badger et al. 1980, Kaplan & Reinhold 1999, Tchernov et al. 2001, 2003). Changes in the $CO_2:HCO_3^-$ uptake ratio are species dependent and occur when very large changes in external CO_2 concentration are imposed (36, 180, 360 and 1800 ppmv) (Burdon 1993, Burkhardt et al. 2001).

Irradiance effects on ε_p

In the present study, increasing light intensities between approximately 1 and 23 µmol photons m^{-2} s^{-1} at constant temperature ($T = 18°C$) resulted in a lower ε_p value, suggesting a heavier Ci pool at higher irradiance values (Fig. 4). This result is at odds with earlier reports (Thompson & Calvert 1995, Rost et al. 2002), and our correlation between irradiance and ε_p might be attributable to the effect of concomitant changes in the $CO_2:HCO_3^-$ uptake ratio and the refreshment of the DIC pool. (Tchernov et al. 1997, 2003). As more light is absorbed, more HCO_3^- is taken up by the algae, a phenomenon demonstrated by a net efflux of CO_2 and HCO_3^- uptake in *E. huxleyi* under very high irradiance (Tchernov et al. 2003).

In contrast, ^{13}C-rich dissolved carbon is cycled out of the cell through the light-dependent MCC; thus, the integrated effect of these processes may control ε_p. We postulate that with increasing light levels, HCO_3^- becomes more dominant as a carbon source for photosynthesis, as shown in Tchernov et al. (2003). In nutrient-limited chemostat studies, such as those described by Laws et al. (1995, 1998), growth rates are controlled by nutrient availability, and it is difficult to achieve high growth rates in the cultures before reaching washout conditions. In contrast, high growth rates may be achieved in batch culture studies (Burkhardt et al. 1999a, Rost et al. 2002, Brutemark et al. 2009). Rost et al. (2002) compared their batch culture results with chemostat data obtained by Bidigare et al. (1997). Growth rates from Bidigare et al. (1997) were between 0.2 and 0.6 d^{-1} compared with 0.5–1.1 d^{-1} in Rost et al. (2002), showing only a slight overlap. Another substantial difference is the light regime applied in the different systems. In chemostat cultures, constant light was used, whereas a light:dark cycle was applied to the batch cultures. In our turbidostat system, we used nutrient-replete media and growth rates were controlled by varying irradiance levels. The growth rates obtained from the turbidostat cultures varied from 0.1 to 1.4 d^{-1} and fall within the range reported in previous studies (Fig. 5).

In constant light treatments, ε_p values are notably higher than under a light:dark cycle (Burkhardt et al. 1999a, Rost et al. 2002). We postulate that these marked differences (8‰; Burkhardt et al. 1999a, Rost et al. 2002; and 6‰; Burkhardt et al. 1999b) are due to the constant dilution of the DIC pool in the algae. Assuming that MCC rates are higher than the saturated photosynthetic rates under a given PFD in a steady state, the depletion of the DIC pool from heavy isotopes is directly correlated with the photoperiod. As the DIC pool, which is the substrate for carboxylation, becomes lighter, so does the organic carbon produced from it. The limiting factor is the specific growth rate (μ_i) relative to the replenishment of the chemostat with DIC by dilution with 'fresh' medium.

A MODEL OF $\delta^{13}C$ ISOTOPIC FRACTIONATION

Model paramaterization

The ratio of ^{13}C to ^{12}C in a sample is denoted as R_{sample}. This measure is usually reported relative to the PDB standard and reported as a δ value (‰):

$$\delta^{13}C_{sample} = 1000 (R_{sample} - R_{PDB})/R_{PDB} \qquad (3)$$

Processes that affect the isotopic composition of a pool of carbon, or that move carbon from one pool to another, such as carbon fixation using RuBisCO, alter these δ values, and are commonly described by an ε notation. We define ε_{AB} as the relative change in isotope ratios between 2 pools, A and B:

$$\varepsilon_{AB} \ = \ 1000 \ (R_A - R_B)/R_A \tag{4}$$

where the convention is that the process moves carbon from A to B. The effect of 2 successive processes can be combined to form an overall conversion factor. Successive processes are multiplicative, so the appropriate combination rule is:

$$(1 - \varepsilon_{AC}/1000) \ = \ (1 - \varepsilon_{AB}/1000) \ (1 - \varepsilon_{BC}/1000) \tag{5}$$

but because the ε values are usually very small compared with 1000, this is usually simplified to the approximate rule:

$$\varepsilon_{AC} = \varepsilon_{AB} + \varepsilon_{BC} \tag{6}$$

A similar simplification is possible for the δ expression for ε_{AB}. While ε_{AB} is usually written as:

$$\varepsilon_{AB} \ = \ (\delta_A - \delta_B)/(1 + \delta_A/1000) \tag{7}$$

the analogous simplification is to write:

$$\varepsilon_{AB} \ = \ \delta_A - \delta_B \tag{8}$$

These simplifications introduce extremely minor errors, which are much less than the uncertainty in the input δ data, and are important because they greatly simplify the expressions needed to describe the isotopic fractionation of carbon in photosynthesis.

The model derivation is a standard mass-balance approach, and Farquhar et al. (1982) and Laws et al. (2002) utilized similar approaches. We decompose the isotopic fractionation due to photosynthesis, ε_p, into 2 stages: the movement of carbon from the extracellular (Ce) environment to the intracellular (Ci) environment and then into organic (org) carbon (but before respiration):

$$\varepsilon_p \ = \ \varepsilon_{Ce,Ci} + \varepsilon_{Ci,org} \tag{9}$$

Alternatively, this can be described as the difference in isotopic composition between extracellular inorganic carbon and fixed organic carbon:

$$\varepsilon_p \ = \ \delta_{Ce} - \delta_{org} \tag{10}$$

using the abbreviation $\delta^{13}C_{org} = \delta_{org}$ and analogous forms (see Table 2 for notation). The isotopic composition of extracellular inorganic carbon is known, although the equilibrium between CO_2(aq) and HCO_3^- will depend on temperature. Some authors measure ε_p relative to CO_2(aq) and not DIC, but we prefer this convention.

The isotopic composition of organic matter δ_{org} depends on the composition of the intracellular pool and the fractionation of carbon fixation:

$$\delta_{org} \ = \ \delta_{Ci} - \varepsilon_{Ci,org} \tag{11}$$

Table 2. Constants describing fractionation process (see text and Eqs. 3–15). The relative change in isotope ratios as C moves from Pool A to B is $\varepsilon_{A,B}$ where A, B are one of Ce, CO_2, HCO_3, CO_2, Ci, org for extracellular inorganic carbon, CO_2(aq), HCO_3^-, intracellular inorganic carbon, and fixed organic carbon, respectively. The isotopic fractionation for select processes is ε_k where k is one of efflux, MCC, or p (organic carbon fixation from extracellular inorganic carbon). The $\delta^{13}C$ for extracellular DIC relative to the PDB standard is δ_{Ce}. MCC: massive carbon cycling; RuBisCo: Ribulose 1,5-bisphosphate carboxylase

Symbol	Process	Range of values (‰)	Our value (‰)
$\varepsilon_{Ce,CO2}$	Chemical	–7 to –10	Temp. function
$\varepsilon_{Ce,HCO3}$	Chemical		0
$\varepsilon_{CO2,Ci}$	Chemical		0
$\varepsilon_{HCO3,Ci}$	Chemical		0
ε_{efflux}	Efflux		1
ε_{MCC}	MCC		1
$\varepsilon_{Ci,org}$	RuBisCO	–21 to –30	27
δ_{Ce}			0
ε_p		–16 to –27	Predicted by model

The composition of the intracellular pool depends on the processes that regulate it, i.e. uptake, efflux and MCC:

$$\delta_{Ci} \ = \ \delta_{Ce} - \varepsilon_{Ce,Ci} + f_{efflux} \, \varepsilon_{efflux} + f_{MCC} \, \varepsilon_{MCC} + \\ (1 - f_{efflux} - f_{MCC}) \, \varepsilon_{Ci,org} \tag{12}$$

The fractionation due to uptake of inorganic carbon into the intracellular pool, $\varepsilon_{Ce,Ci}$, is complicated by the potential variation among passive diffusion and active uptake as well as the preference for CO_2 over bicarbonate:

$$\varepsilon_{Ce,Ci} \ = \ f_{CO2,diff}(\varepsilon_{Ce,CO2} + \varepsilon_{CO2,Ci,diff}) + f_{CO2,active}(\varepsilon_{Ce,CO2} \\ + \varepsilon_{CO2,Ci,active}) + f_{HCO3,active}(\varepsilon_{Ce,HCO3} + \varepsilon_{HCO3,Ci}) \tag{13}$$

Combining Eqs. (9–13), we obtain the overall fractionation factor:

$$\varepsilon_p \ = \ f_{CO2,diff}(\varepsilon_{Ce,CO2} + \varepsilon_{CO2,Ci,diff}) + f_{CO2,active}(\varepsilon_{Ce,CO2} + \\ \varepsilon_{CO2,Ci,active}) + f_{HCO3,active}(\varepsilon_{Ce,HCO3} + \varepsilon_{HCO3,Ci}) - f_{efflux} \\ \varepsilon_{efflux} - f_{MCC} \, \varepsilon_{MCC} + (f_{efflux} + f_{MCC})\varepsilon_{Ci,org} \tag{14}$$

A simplified form can be used if we discount small fractionation terms:

$$\varepsilon_p \ = \ (f_{CO2,diff} + f_{CO2,active})\varepsilon_{Ce,CO2} - f_{efflux} \, \varepsilon_{efflux} - \\ f_{MCC} \, \varepsilon_{MCC} + (f_{efflux} + f_{MCC}) \, \varepsilon_{Ci,org} \tag{15}$$

This is consistent with the commonly used linear relationship between ε_p and μ:$[CO_2]$ if we assume that f_{efflux} and f_{MCC} are constant in addition to the usual assumptions of constant carbon quota, constant cell membrane permeability and uptake of inorganic carbon only by passive diffusion.

Changes in temperature lead to changes in chemical reaction rate constants governing equilibria in the carbonate system. We use a greatly simplified version that only includes a quadratic dependence on temperature. This relationship predicts $[CO_2(aq)]$ as a function of T (in °C):

$$[CO_2(aq)] \; = \; 22.36 - 0.7161\,T + 0.0097\,T^2 \quad (16)$$

and is consistent with our experimental data and simplified carbonate chemistry equations. Temperature changes also affect the isotopic composition of extracellular CO_2 because of the increase in CO_2 solubility:

$$\delta^{13}C_{CO2} = \delta^{13}C_{DIC} + 23.644 - 9701.5/(T + 273.15) \quad (17)$$

Phytoplankton uptake of CO_2 and HCO_3^- depends on temperature and $[CO_2(aq)]$ because of changes in diffusion, extracellular concentrations of carbon species and the activity of a CCM. Uptake of CO_2 by diffusion into the cell is:

$$V_{CO2,diff} \; = \; -4\pi RD \, (C_0 - [CO_2(aq)]) \quad (18)$$

where C_0 is the concentration of CO_2 at the cell surface, R is the radius of the cell and D is the temperature-dependent diffusion constant. Changes in $[CO_2(aq)]$ will result in a linear response in the diffusion uptake. The temperature dependence of D is linear, but ignored because the variability is much less than the corresponding changes in $[CO_2(aq)]$.

Active uptake is conveniently modeled by a Michaelis-Menten function for both CO_2 and HCO_3^-. Uptake of CO_2 is for the most part subsaturating and can be described by a linear response to environmental CO_2 or by the more complete saturating function. Bicarbonate uptake is saturated and shows essentially no variability over the range of experimental conditions considered. The CCM is activated at low $[CO_2]$ when a higher percentage of DIC uptake is of HCO_3.

Active uptake of CO_2 and HCO_3 depends directly on extracellular CO_2 and HCO_3^- and indirectly on temperature according to:

$$V_{CO2,active} \; = \; 260 \, [CO_2]/([CO_2] + 13.4) \quad (19)$$

and

$$V_{HCO3^-,active} \; = \; 58 \quad (20)$$

where $[CO_2]$ is in $\mu mol \, l^{-1}$ and uptake is in $\mu mol \, mg^{-1}$ chl a h^{-1} (Rost et al. 2002). The numerical values are used here only for convenience. In fact, we know very little about the relative uptake of CO_2 and HCO_3^-. The feature of primary importance is that $a = V_{CO2}/V_{HCO3^-}$ decreases as $[CO_2]$ decreases and temperature increases.

Loss terms are much more difficult to quantify than uptake, so we aim to include only the most obvious qualitative features into our model. Under steady-state conditions, efflux must be less than uptake. Since increasing temperature is associated with decreasing carbon uptake by passive diffusion, we argue that efflux will also decrease as a fraction of uptake to permit carbon fixation to continue or increase. The second derivative of efflux is positive; as efflux decreases towards 0, we expect the rate of decrease to attenuate. A function consistent with these observations is:

$$f_{efflux} \; = \; 1/10 + 3/4 \, [(T - 33)/33]^4 \quad (21)$$

which is 0.85 at $T = 0$ and declines to 0.1 at $T = 33$.

MCC is turned on at the same time as the CCM. Evidence suggests that amount of MCC increases rapidly with decreasing $[CO_2]$ and CCM activity. For MCC, we assume that the level is close to 0 below a threshold temperature, $T_{MCC} = 13$°C, and increases to approximately 80% of the uptake rate at the upper end of the temperature range suitable for growth. One possible definition is

$$f_{MCC} \; = \; \exp[(T - 37)/14] \quad (22)$$

The fraction of DIC taken into the cell that goes to growth is $f_\mu = 1 - f_{efflux} - f_{MCC}$. An alternative formulation could use growth rate to constrain efflux and MCC further. It must be noted that this growth rate refers only to carbon fixed, does not include respiration or other loss terms, and may be only loosely related to net photosynthesis and growth.

Comparison of the observed results and model outputs

We suggest that ε_p values for *Emiliania huxlei* reflects both temperature and pCO_2 conditions at constant light intensities. These parameters influence ε_p through transient MCC and CCM activity, and the sensitivity of ε_p to changes in MCC, CCM, $[CO_2]$ and temperature is predicted by our model (Fig. 6).

In contrast to previous studies, we believe that under our experimental conditions, elevated light intensities only slightly effected POC isotopic composition and that POC became slightly richer with ^{13}C. This is possibly based on the capability of photosynthetic organisms to change the ratio of CO_2:HCO_3^- uptake (Burkhardt et al. 2001, Tchernov et al. 2003). This ratio sets the basic isotopic composition of the Ci pool, which serves as the substrate for carboxylation. The constant conversion of CO_2 to HCO_3^- against the
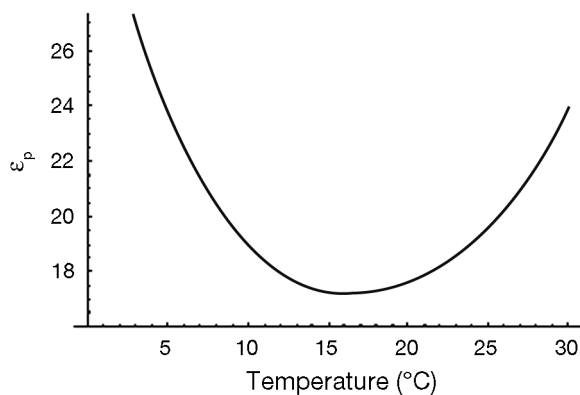
Fig. 6. The simulation model output of the relationship between isotopic fractionation during carbon fixation (ε_p) and temperature. The parameters used for this simulation are shown in Table 2
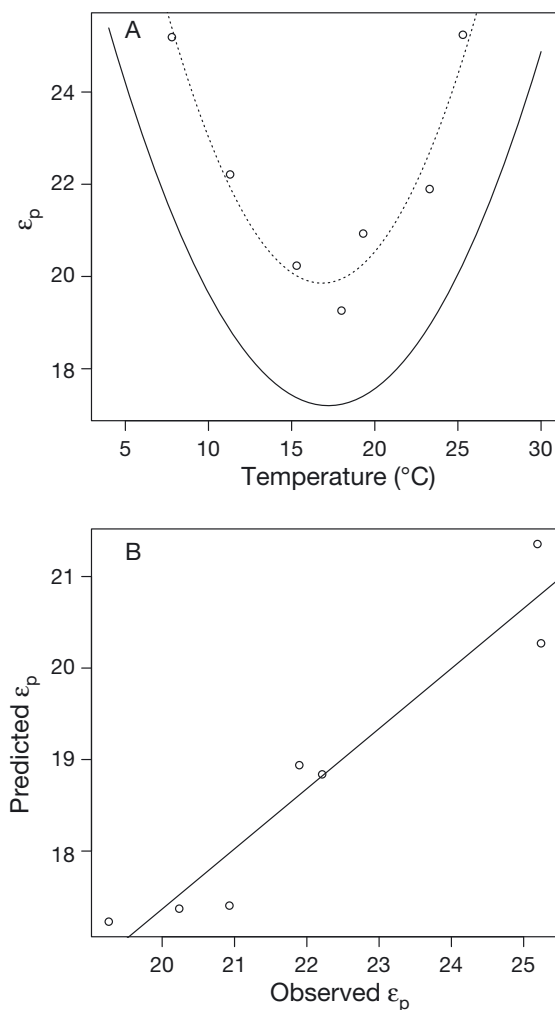

Fig. 7. (A) Relationship between isotopic fractionation during carbon fixation (ε_p) and temperature. The data with a quadratic fit (dotted line) are compared with the model outcome (solid line). (B) Comparison of the observed ε_p with the predicted ε_p for the same temperature

physical chemical equilibrium under low CO_2 conditions will, with little doubt, minimize the leakage of CO_2 from the cytoplasm and thus cause a deviation from the Ci species-dependent expected equilibrium of $\delta^{13}C$ under equilibrium conditions (O'Leary 1981). Our data reveal that the isotopic composition of the Ci pool is a crucial component that determines to a great extent the isotopic composition of the photosynthetic product, as originally suggested by Sharkey & Berry (1985).

Our experimental results and model suggest that massive inorganic carbon cycling may strongly influence the isotopic composition of POC. MCC might have a large effect on the $\delta^{13}C$ of photosynthetic products of calcareous phytoplankton species such as *E. huxleyi* under different environmental conditions, such as light and temperature.

To further explore the U-shaped dependence of ε_p on temperature and [CO_2(aq)] (Fig. 3), we developed a numerical simulation model that uses the following state variables: the CO_2:HCO_3^- uptake ratio (which depends on temperature as it affects the relative abundance of carbonate species in seawater), diffusion, and active uptake kinetics of inorganic carbon. This effect is manifested by differential fractionation of carbon as passive diffusion of [CO_2(aq)] decreases when temperature increases. In addition, the isotopic composition of the Ci pool changes due to efflux of inorganic carbon, the activity of the CCM and associated MCC. The novel feature of our model is the prediction that ε_p increases (more ^{12}C is incorporated into organic matter) as the CCM and MCC become activated at low [CO_2(aq)] and high growth rates (Fig. 6). It predicts the same quadratic variation in ε_p as a function of temperature as observed experimentally. It is noted that the model predictions are lower than the data by 2–5‰, but are linearly related to the observations (R^2 = 0.90, p < 0.001; Fig. 7). These results indicate that MCC is likely to have a major impact on the $\delta^{13}C$ composition of the photosynthetic products of *E. huxleyi*. A better understanding of how each individual process influences the end product will indeed bring us closer to a unified model that would enable us to try and reconstruct paleo-CO_2 concentrations through $\delta^{13}C$ analysis.

LITERATURE CITED

Badger MR (1987) The CO_2-concentrating mechanism in aquatic phototrophs. In: MD Hatch, NK Boardman (eds) The biochemistry of plants: a comprehensive treatise, Vol 10. Photosynthesis. Academic Press, New York, NY, p 219–274

Badger MR, Kaplan A, Berry JA (1978) A mechanism for concentrating CO_2 in *Chlamydomonas reinhardtii* and *Anabaena variabilis* and its role in photosynthetic CO_2 fixation. Year B Carnegie Inst Wash 77:251–261

Badger MR, Kaplan A, Berry JA (1980) Internal inorganic carbon pool of *Chlamydomonas reinhardtii*: evidence for a carbon dioxide-concentrating mechanism. Plant Physiol 66:407–413

Badger MR, Palmqvist K, Yu JW (1994) Measurement of CO_2 and HCO_3^- fluxes in cyanobacteria and microalgae during steady-state photosynthesis. Physiol Plant 90: 529–536

Bidigare RR, Fluegge A, Freeman KH, Hanson KL and others (1997) Consistent fractionation of ^{13}C in nature and in the laboratory: growth-rate effects in some haptophyte algae. Global Biogeochem Cycles 11:279–292

Bolton CT, Stoll HM, Mendez-Vicente A (2012) Vital effects in coccolith calcite: Cenozoic climate-pCO2 drove the diversity of carbon acquisition strategies in coccolithophores? Paleoceanography 27:PA4204

Brutemark A, Lindehoff E, Graneli E, Graneli W (2009) Carbon isotope signature variability among cultured microalgae: influence of species, nutrients and growth. J Exp Mar Biol Ecol 372:98–105

Burdon RH (1993) Stress proteins in plants. Bot J Scotl 46: 463–475

Burkhardt S, Riebesell U, Zondervan I (1999a) Effects of growth rate, CO_2 concentration, and cell size on the stable carbon isotope fractionation in marine phytoplankton. Geochim Cosmochim Acta 63:3729–3741

Burkhardt S, Riebesell U, Zondervan I (1999b) Stable carbon isotope fractionation by marine phytoplankton in response to daylength, growth rate, and CO_2 availability. Mar Ecol Prog Ser 184:31–41

Burkhardt S, Amoroso G, Riebesell U, Sultemeyer D (2001) CO_2 and HCO_3^- uptake in marine diatoms acclimated to different CO_2 concentrations. Limnol Oceanogr 46: 1378–1391

Edvardsen B, Eikrem W, Green JC, Andersen RA, Moon-van der Staay SY, Medlin LK (2000) Phylogenetic reconstructions of the Haptophyta inferred from 18S ribosomal DNA sequences and available morphological data. Phycologia 39:19–35

Espie GS, Canvin DT (1987) Evidence for Na⁺-independent HCO_3^- uptake by the cyanobacterium *Synechococcus leopoliensis.* Plant Physiol 84:125–130

Espie GS, Kandasamy RA (1992) Na⁺-independent HCO_3^- transport and accumulation in the cyanobacterium *Synechococcus* UTEX 625. Plant Physiol 98:560–568

Falkowski PG (1984a) Kinetics of adaptation to irradiance in *Dunaliella tertiolecta.* Photosynthetica 18:62–68

Falkowski PG (1984b) Physiological responses of phytoplankton to natural light regimes. J Plankton Res 6: 295–307

Farquhar GD, O'Leary MH, Berry JH (1982) On the relationship between carbon isotope discrimination and the intercellular carbon dioxide concentration in leaves. Aust J Plant Physiol 9:121–137

Freeman KH, Hayes JH (1992) Fractionation of carbon isotopes by phytoplankton and estimates of ancient CO_2 levels. Global Biogeochem Cycles 6:185–198

Guillard RRL, Ryther JH (1962) Studies of marine planktonic diatoms. I. *Cyclothella nana* (Hustedt) and *Detonula confervacea* (Cleve). Can J Microbiol 8:229–239

Huertas IE, Espie GS, Colman B, Lubian LM (2000a) Light-dependent bicarbonate uptake and CO_2 efflux in the marine microalga *Nannochloropsis gaditana.* Planta 211: 43–49

Huertas IM, Colman B, Espie GS, Lubian LM (2000b) Active transport of CO_2 by three species of marine microalgae. J Phycol 36:314–320

Iglesias-Rodriguez MD, Brown CW, Doney SC, Kleypas J and others (2002) Representing key phytoplankton functional groups in ocean carbon cycle models: Coccolithophorids. Global Biogeochem Cycles 16:47–1/47–20, doi: 10.1029/2001GB00145

Jasper JP, Hayes JM (1990) A carbon isotope record of CO_2 levels during the late quaternary. Nature 347:462–464

Kaplan A (1981) Photoinhibition in *Spirulina platensis*: response of photosynthesis and HCO_3^- uptake capability to CO_2 depleted conditions. J Exp Bot 32:669–677

Kaplan A, Reinhold L (1999) The CO_2 concentrating mechanisms in photosynthetic microorganisms. Annu Rev Plant Physiol Plant Mol Biol 50:539–570

Kaplan A, Badger MR, Berry JA (1980) Photosynthesis and intracellular inorganic carbon pool in the blue-green algae *Anabaena variabilis*: response to external CO_2 concentration. Planta 149:219–226

Keller K, Morel FMM (1999) A model of carbon isotopic fractionation and active carbon uptake in phytoplankton. Mar Ecol Prog Ser 182:295–298

Laws EA, Popp BN, Bidigare RR, Kennicutt MC, Macko SA (1995) Dependence of phytoplankton carbon isotopic composition on growth rate and CO_2: theoretical considerations and experimental results. Geochim Cosmochim Acta 59:1131–1138

Laws EA, Popp BN, Bidigare RR (1997) Effect of growth rate and CO_2 concentration on carbon isotopic fractionation by the marine diatom *Phaeodactylum tricornutum.* Limnol Oceanogr 42:1552–1560

Laws EA, Thompson PA, Popp BN, Bidigare RR (1998) Sources of inorganic carbon for marine microalgal photosynthesis: a reassessment of $\delta^{13}C$ data from batch culture studies of *Thalassiosira pseudonana* and *Emiliania huxleyi.* Limnol Oceanogr 43:136–142

Laws EA, Popp BN, Cassar N, Tanimoto J (2002) ^{13}C discrimination patterns in oceanic phytoplankton: the likely influence of CCMs and the implications for palaeoreconstructions. Funct Plant Biol 29:323–333

Lucas WJ (1978) HCO_3^- influx across the plasmalemma of *Chara corallina.* Plant Physiol 61:487–493

Lucas WJ, Nuccitelli R (1980) HCO_3^- and OH^- transport across the plasmalemma of *Chara.* Planta 150:120–131

Miller AG, Colman B (1980) Evidence for HCO_3^- transport by the blue-green alga (cyanobacterium) *Coccochloris peniocystis.* Plant Physiol 65:397–402

Nimer NA, Merrett MJ (1996) The development of a CO_2-concentrating mechanism in *Emiliania huxleyi.* New Phytol 133:383–389

Nimer NA, Dong LF, Guan Q, Merrett MJ (1995) Calcification rate, dissolved inorganic carbon utilization and carbonic anhydrase activity in *Emiliania huxleyi.* Bull Inst Oceanogr 0:43–49

O'Leary MH (1981) Carbon isotope fractionation in plants. Phytochemistry 20:553–567

Pagani M, Arthur MA, Freeman KH (1999) Miocene evolution of atmospheric carbon dioxide. Paleoceanography 14:273–292

Pagani M, Freeman KH, Ohkouchi N, Caldeira K (2002) Comparison of water column [CO_2(aq)] with sedimentary alkenone-based estimates: a test of the alkenone-CO_2 proxy. Paleoceanography 17:21-1–21-12

Post AF, Dubinsky Z, Wyman K, Falkowski PG (1984) Kinetics of light-intensity adaptation in a marine planktonic diatom. Mar Biol 83:231–238

Rau GH (1994) Variations in sedimentary organic d^{13}C as a proxy for past changes in ocean and atmospheric [CO_2]. Paper presented at: Carbon Cycling in the Glacial Ocean: Constraints on the Ocean's Role in Global Climate Change. Berlin, Springer, p 307–322

Rau GH, Des Marais David J, Oremland RS (1982) Stable isotope abundance in sedimentary inorganic, organic, and pigment carbon; application to aquatic paleoecology. Eos Trans AGU 63:957

Raven JA, Giordano M, Beardall J, Maberly SC (2011) Algal and aquatic plant carbon concentrating mechanisms in relation to environmental change. Photosynth Res 109:281–296

Raven JA, Giordano M, Beardall J, Maberly SC (2012) Algal evolution in relation to atmospheric CO_2: carboxylases, carbon-concentrating mechanisms and carbon oxidation cycles. Philos Trans R Soc B Biol Sci 367:493–507

Riebesell U, Burkhardt S, Dauelsberg A, Kroon B (2000) Carbon isotope fractionation by a marine diatom: dependence on the growth-rate-limiting resource. Mar Ecol Prog Ser 193:295–303

Rost B, Zondervan I, Riebesell U (2002) Light-dependent carbon isotope fractionation in the coccolithophorid *Emiliania huxleyi.* Limnol Oceanogr 47:120–128

Rost B, Riebesell U, Sultemeyer D (2006) Carbon acquisition of marine phytoplankton: effect of photoperiod length. Limnol Oceanogr 51:12–20

Sekino K, Shiraiwa Y (1994) Accumulation and utilization of dissolved inorganic carbon by a marine unicellular coccolithophorid, *Emiliania huxleyi.* Plant Cell Physiol 35:353–361

Sekino K, Kobayashi H, Shiraiwa Y (1996) Role of coccoliths in the utilization of inorganic carbon by a marine unicellular coccolithophorid, *Emiliania huxleyi*: a survey using intact cells and protoplasts. Plant Cell Physiol 37:123–127

Sharkey TD, Berry JA (1985). Carbon isotope fractionation of algae as influenced by inducible CO_2 concentrating mechanism. In: Lucas WJ and Berry JA (eds) Inorganic carbon uptake by aquatic photosynthetic organisms. American Society of Plant Physiologists, Rockville, MD, p 389–340

Shiraiwa Y (2003) Physiological regulation of carbon fixation in the photosynthesis and calcification of coccolithophorids. Comp Biochem Physiol B 136:775–783

Stoll HM, Klaas CM, Probert I, Encinar JR, Alonso JIG (2002) Calcification rate and temperature effects on Sr partitioning in coccoliths of multiple species of coccolithophorids in culture. Global Planet Change 34:153–171

Sukenik A, Bennett J, Falkowski P (1987) Light-saturated photosynthesis—limitation by electron transport or carbon fixation. Biochim Biophys Acta 891:205–215

Sukenik A, Tchernov D, Huerta E, Lubian LM, Kaplan A, Livne A (1997) Uptake, efflux and photosynthetic utilization of inorganic carbon by the marine eustigmatophyte *Nannochloropsis* sp. J Phycol 33:969–974

Tchernov D, Hassidim M, Luz B, Sukenik A, Reinhold L, Kaplan A (1997) Sustained net CO_2 evolution during photosynthesis by marine microorganisms. Curr Biol 7:723–728

Tchernov D, Helman Y, Keren N, Luz B and others (2001) Passive entry of CO_2 and its energy-dependent intracellular conversion to HCO_3^- in cyanobacteria are driven by a photosystem I-generated μH^+. J Biol Chem 276:23450–23455

Tchernov D, Silverman J, Luz B, Reinhold L, Kaplan A (2003) Massive light-dependent cycling of inorganic carbon between oxygenic photosynthetic microorganisms and their surroundings. Photosynth Res 77:95–103

Thompson PA, Calvert SE (1995) Carbon isotope fractionation by *Emiliania huxleyi.* Limnol Oceanogr 40:673–679

Tortell PD, Morel FMM (2002) Sources of inorganic carbon for phytoplankton in the Eastern Subtropical and Equatorial Pacific Ocean. Limnol Oceanogr 47:1012–1022

Volokita M, Zenvirth D, Kaplan A, Reinhold L (1984) Nature of the inorganic carbon species actively taken up by the cyanobacterium *Anabaena variabilis.* Plant Physiol 76:599–602

Wolf-Gladrow D, Riebesell U (1997) Diffusion and reactions in the vicinity of plankton: a refined model for inorganic carbon transport. Mar Chem 59:17–34

Wolf-Gladrow D, Riebesell U, Burkhardt S, Bijma J (1999) Direct effects of CO_2 concentration on growth and isotopic composition of marine plankton. Tellus B Chem Phys Meterol 51:461–476